PHYSICAL REVIEW B VOLUME 31, NUMBER 6 15 MARCH 1985

Far-infrared transmittance of boron-implanted germanium at liquid-helium temperatures

V. Hadek, D. M. Watson,* and C. A. Beichman
Jet Propulsion Laboratory, California Institute of Technology, Pasadena, California 91109

M. D. Jack
Carlsbad Technology Center, Hughes Aircraft Company, Carlsbad, California 92008
(Received 10 September 1984; revised manuscript received 13 November 1984)

The transmission of far-infrared radiation of 100-μm wavelength through Ge wafers ion implanted with B was measured at a temperature of approximately 4 K. Transmittance ranged from approximately 0.5 to 0.08 for doses from 3×10^{12} to 3×10^{15} cm^{-2}. The resistivity at temperatures between 4 and 1 K, and the impurity profiles of the implanted layers were also measured and correlated with the infrared transmittance.

INTRODUCTION

We have measured the transmission of far-infrared radiation of 100-μm wavelength through liquid-helium temperature Ge wafers which have an ion-implanted layer of B near one surface. Our interest in this arises from the possible use of such implanted layers as contacts for infrared detectors which would be illuminated through these contact layers rather than by the conventional method of side illumination. For such an application we need to know if the contact layer is sufficiently transparent to infrared that the detector sensitivity will not be significantly reduced.

SPECIMEN DESCRIPTION

The wafers were Ge, 0.5 mm thick and 50 mm in diameter, single crystal [100], undoped before implantation. Except for a control wafer, No. 9, they were ion implanted with B at energies and doses given in Table I. After implant each wafer was separated into four quadrants, each of which received a different annealing treatment as given in Table II, except for wafer No. 8 which only received annealing treatment *A*. From each quadrant a piece 9 mm square was cut for the infrared transmission measurement and also a strip approximately 2.5 mm wide by 25 mm long for the low-temperature resistivity measurement. To determine the distribution profile of the implanted B as a function of depth, spreading resistance measurements were made. According to these measurements, the implanted layer extended typically to a depth of about 0.2 μm.

TABLE I. Implant parameters for wafers.

Specimen identification	Implant energy (keV)	B dose (cm^{-2})
No. 2	10	3×10^{15}
No. 3	10	1×10^{15}
No. 4	10	3×10^{14}
No. 5	20	1×10^{14}
No. 6	20	3×10^{13}
No. 7	20	1×10^{13}
No. 8	20	3×10^{12}
No. 9 (control)	not implanted	

OPTICAL MEASUREMENTS

The far-infrared transmission of each ion-implanted germanium specimen was measured at a temperature of approximately 4 K by use of a low-background detector-testing system, diagrammed in Fig. 1. This system occupied the work surface of a commercial liquid-nitrogen-jacketed helium dewar, and consisted of a Ge:Ga photoconductive detector,[1] a junction field-effect transistor (JFET) preamplifier maintained at 100 K,[2] a series of filters which defined a 0.8-μm band centered at $\lambda=100.0$ μm, and a wheel used to rotate specimens in and out of the beam. The bandpass filter[3] was a metal-mesh Fabry-Perot interferometer set in first order at $\lambda=100$ μm; the higher orders of this filter were rejected by a combination of salt reststrahlen filters (BaF_2 and KCl), diamond dust, and black polyethylene. Radiation shields and baffles ensured that all components, including the Ge specimens being measured, were near the temperature of the liquid-helium bath. A room-temperature chopper and liquid-nitrogen-temperature cold load outside of the Dewar provided the infrared signal.

TABLE II. Annealing parameters for wafer quadrants.

Quadrant identification	Anneal temperature (°C)	Anneal time (min)
A	550	10
B	550	3
C	500	12
D	500	3

 ©1985 The American Physical Society

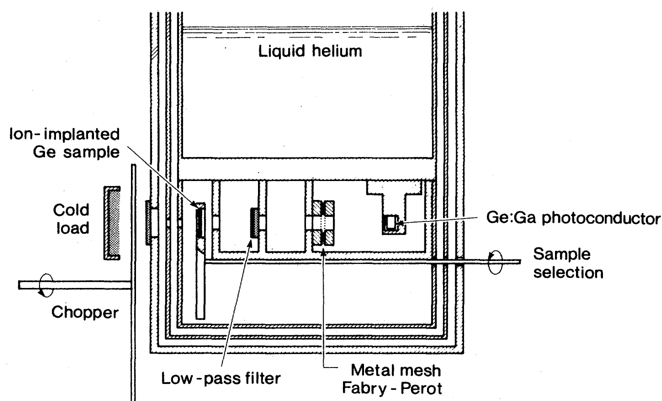

FIG. 1. Diagram of the experimental apparatus system used to measure the far-infrared transmission of the ion-implanted Ge specimens.

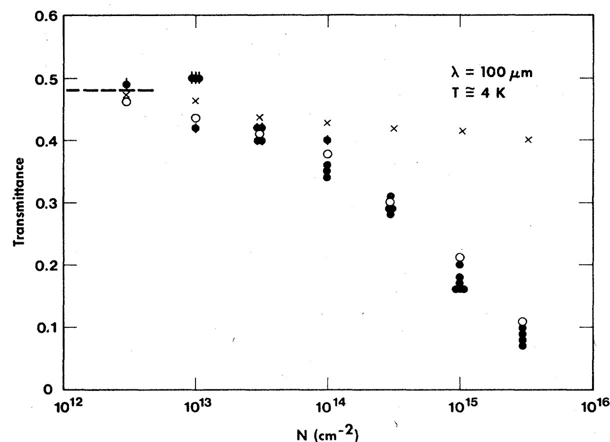

FIG. 2. Far-infrared transmittance of the ion-implanted Ge specimens. The horizontal dashed line indicates the transmittance of the unimplanted germanium control specimen (No. 9). Solid circles are experimental data, crosses are calculated transmittance using $m^* = 0.3m_e$; open circles are calculated using $m^* = 0.075m_e$.

The transmission of each specimen was measured relative to a clear aperture, a blocked aperture, and the control specimen, No. 9, which had not been ion implanted but was otherwise identical to the implatned ones. The reproducibility of the transmitted signal was $\pm 1\%$. Results are given in Fig. 2.

ELECTRICAL MEASUREMENTS

Four-terminal resistivity measurements were performed using approximately 500-Hz ac. For this measurement, each 2.5 mm$\times$25 mm strip of Ge described earlier was cleaned and etched to remove any oxide, and four 0.05-mm-diameter Au wires were immediately soldered with In to it. The specimens were mounted only by means of the wires to avoid stress, and immersed in a liquid-helium bath. Care was taken to exclude light since the resistance of the specimens was slightly light sensitive. Reduced data are given in column 4 of Table III. Within experimental uncertainty there were no differences in resistivity among the specimens receiving the four different annealing treatments. Specimens 3*A*, 4*A*, 5*A*, 6*A*, 6*D*, 7*A*, 7*D*, and 8*A* were also measured at temperatures down to approximately 1.2 K; there was no change in resistance from the values at 4.2 K.

From the temperature dependence of the resistivity data we conclude that all implanted specimens were degenerately doped. However, this is not in agreement with the concentrations determined by the spreading resistance measurements.

The values of the impurity concentration, *N*, can be estimated from the total ion flux and the thickness of the doped layer, in other words, the penetration depth of the ions. Using the concentration profile obtained from the spreading resistance data, and the approximation that the impurity concentration is equal to the total flux divided by the half-width *d* of the profile curve, we obtain concentrations which are somewhat higher than those obtained from the spreading resistance. The comparison is shown in Table III. We are uncertain at present of the exact reason for the discrepancy between the two sets of values for the impurity concentration, *N*. Possible reasons are (a) that not all implanted ions become electrically active and (b) that, due to residual damage after annealing, the concentration versus conductivity dependence in the implanted material is different from that in conventionally doped material. The first reason would make the

TABLE III. Experimental results and calculations. The last two columns are theoretical values of the transmittance *T*. Column 5 uses the effective mass of the heavy holes to characterize the valence-band structure, the sixth column uses a quarter of that mass.

Specimen identification	*N* from half-width (cm^{-3})	*N* from flux/half-width (cm^{-3})	σ_0 (Ω^{-1}cm^{-1})	*T* ($m^*=0.3m_e$)	*T* ($m^*=0.075m_e$)
2*A*	4×10^{19}	3.7×10^{20}	2×10^{3}	0.403	0.104
3*A*	2×10^{19}	2×10^{20}	1×10^{3}	0.427	0.190
4*A*	3×10^{18}	3.7×10^{19}	5.3×10^{2}	0.426	0.281
5*A*	7×10^{17}	1.5×10^{19}	2.1×10^{2}	0.428	0.374
6*A*	2×10^{17}	3×10^{18}	78	0.434	0.425
7*A*	6×10^{16}	1.5×10^{18}	32	0.464	0.430
8*A*	2×10^{16}	3×10^{18}	2.9	0.472	0.460

estimate of N from the total flux too large, the second would make the value of N obtained from the spreading resistance too low. We shall, however, consider the values obtained from the total flux as more realistic, primarily because they are compatible with the well-established concentration for the metal-insulator transition in Ge.[4]

ANALYSIS AND DISCUSSION

Below, we present a theoretical analysis of the transmitivity of 100-μm light through the specimens, and compare the calculated values with our experimental results. For the purpose of the analysis, we take the simplest possible model. Specifically, we make the following assumptions.

(1) The concentration profile is approximated by a step function at the depth d.

(2) The infrared conductivity can be expressed by the Drude formula[5] involving a single relaxation time τ,

$$\sigma(\omega)=\sigma_0/(1+i\omega\tau) , \tag{1}$$

where σ_0 is the dc conductivity.

(3) The density of states (DOS) in the conducting layer corresponds to the usual effective mass of heavy holes,[6] and is given by the Boltzmann expression

$$\sigma_0=\mathrm{N}e\tau/m^* . \tag{2}$$

The effective-mass approximation may be invalid for two reasons: The heavy doping modifies the structure of the valence-band edge,[7] and the doped layer is sufficiently thin for quantum-well effects to be important.[8] These would strongly modify the density of states by splitting the valence band into subbands. However, the likelihood of the subband structure is no doubt diminished by the disorder introduced by the heavy doping. The interplay between the disorder and the quantum-well effects is an interesting problem in itself, but outside the scope of this work. Here, we simply assume that the structure of the valence band is represented by the heavy holes in Ge.

(4) In accordance with the actual structure of our samples, we take the (polished) doped surface of the samples to be smooth, while the (lapped) surface at the undoped end is taken to be "rough." Although this introduces some uncertainty, it was not a serious concern for our purposes since we assumed that its primary effect is on the absolute rather than the relative values of transmittance.

Figure 3 defines the regions of the specimens referred to in the calculations below. Media 1 and 4 are vacuum,

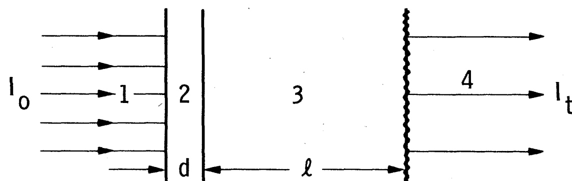

FIG. 3. Definition of regions in Ge wafers for calculations of transmittance.

medium 2 is the doped layer, and medium 3 is the undoped material. I_0 is the intensity of the incident ir illumination and I_t is the intensity of the transmitted ir. We are interested in the transmittance

$$T=I_t/I_0 \tag{3}$$

through the specimen, which we evaluated from the complex Fresnel coefficients r_{ij}, t_{ij} for the three interfaces. For example, r_{12} (t_{12}) is the Fresnel coefficient for reflection (transmission) for light incident from medium 1 onto the surface between media 1 and 2 (surface 12). The Fresnel coefficients r_{ij},t_{ij} are related to the complex refractive indices n_i,n_j by[9]

$$r_{ij}=(n_j-n_i)/(n_j+n_i) , \tag{4}$$

$$t_{ij}=2n_i/(n_j+n_i) . \tag{5}$$

Each refractive index n is in turn related to the complex relative dielectric constant

$$\kappa=\kappa_0+\sigma(\omega)/i\omega\epsilon \tag{6}$$

by

$$n=\sqrt{\kappa} . \tag{7}$$

Here, ϵ is the dielectric constant of vacuum, and κ_0 is the relative dielectric constant of the medium. For undoped germanium, $\kappa_0=16$.

In addition to the above four assumptions, we also assume the following.

(5) In medium 3, the superposition of light transmitted through plane 23 and of light reflected from plane 34 is incoherent, so that we can add intensities rather than amplitudes. This assumption is based on the roughness of the undoped surface, the fact that no attempt has been made to make the surfaces 12 and 34 optically parallel with respect to each other, and the fact that $l \gg \lambda=100$ μm.

(6) We shall, however, still assume that the light after reflection from plane 34 remains predominantly at normal incidence, even after multiple reflections. The assumption is based on the fact that the "transverse" rms roughness of the surface is less than a quarter wavelength, but the "longitudinal" roughness is of a longer scale.

In medium 2, the superposition of the light transmitted through 12 and reflected from 23 (and vice versa) is taken to be coherent. The reason is that d, which we believe to be constant along the surface, obeys $d \ll \lambda$. We denote the transmittivity from region 1 into region 3 through the doped layer by T_{13}, and the reflectivity from the doped layer by R_{13}. Similarly, we denoted by T_{34} the transmittivity through 34 of light incident from medium 3, and by R_{34} the reflectivity from that surface. Note that while $T_{34}=1-R_{34}$, the relation $T_{13}=1-R_{13}$ is generally incorrect. The reasons for the difference are that while the properties R_{34},T_{34} refer to a surface, the properties T_{13} and R_{13} refer to a region of finite thickness. Furthermore, the conductivity in region 2 is finite, thus causing absorption, hence $T_{13}+R_{13}<1$.

The intensity I_t transmitted through the sample can be calculated in terms of the quantities T_{13}, R_{13}, and R_{34},

taking into account all of the multiple reflections. As illustrated in Fig. 4, the total transmittance is obtained as the sum

$$T=\frac{I_t}{I_0}=T_{13}(1-R_{34})+T_{13}R_{34}R_{13}(1-R_{34})$$
$$+T_{13}R_{34}R_{13}R_{34}R_{13}(1-R_{34})+\cdots \quad (8)$$

It is seen by inspection that the right-hand side constitutes an infinite geometric series with the first term as $T_{13}(1-R_{34})$, and a ratio $R_{13}R_{34}$ between successive terms. Thus,

$$T=T_{13}(1-R_{34})/(1-R_{13}R_{34}) . \quad (9)$$

Notice that Fig. 4 as well as Eq. (6) assumes no absorption in layer 3, as appropriate for Ge at infrared frequencies and low temperature.

It remains to evaluate T_{13}, R_{13}, and R_{34} in terms of the material constants. R_{34} can be immediately evaluated as

$$R_{34}=|r_{34}|^2=|(n_4-n_3)/(n_4+n_3)|^2=9/25 . \quad (10)$$

The quantities R_{13} and T_{13} are more difficult to calculate. They must take account of all multiple reflections in layers 2 and 3, as suggested by Fig. 3. However, since the superposition of the waves in region 2 is coherent, the multiple reflections must involve complex amplitudes, to take account of relative phases, rather than intensities.

In terms of the appropriate Fresnel coefficients, the reflection and transmission coefficients r_{13} and t_{13} for amplitudes are[10]

$$r_{13}=(r_{12}+r_{23}a_2^2)/(1+r_{12}r_{23}a_2^2) , \quad (11)$$

$$t_{13}=t_{13}t_{23}a_2^2/(1+r_{12}r_{23}a_2^2) , \quad (12)$$

where $a=\exp(idn_2\omega/c)$, c being light velocity. R_{13} and T_{13} then are

$$R_{13}=r_{13}r_{13}^* , \quad (13)$$

$$T_{13}=t_{13}t_{13}^*n_3/n_1 . \quad (14)$$

Inserting Eqs. (4) and (5) into Eqs. (11) and (12); Eqs. (11) and (12) into Eqs. (13) and (14); and Eqs. (13) and (14) into Eq. (9) gives the desired quantity T in terms of the material constants $n_1=n_4$, n_2, and n_3. Using Eqs. (1) and (2) in Eq. (6), and Eq. (6) in Eq. (7) expresses n in terms of the known quantities κ_0, m^*, and the measured quantities N (impurity concentration) and σ_0 (dc conductivity). One thus obtains T in terms of σ_0, N, m^*, and κ_0. The expression is cumbersome and there is little point in displaying it here. The values of T were computed for the various samples using the value[11] $m^*=0.3m_e$, appropriate for the heavy-hole mass in Ge, $\kappa_0=16$, and the values for κ_0 and N from Table III. The latter values of N were taken from the third column, calculated from the total flux.

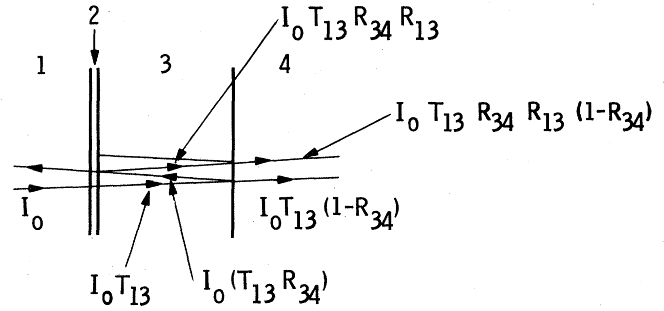

FIG. 4. Intensities of the transmitted and reflected illumination in the various regions, as referred to in the calculations.

The computed values for T are given in the fifth column of Table III, and indicated in Fig. 2 by crosses. It is clearly observed that, while the agreement with experiment is quite good for small values of N, it becomes poor for large N, where the theoretical values are substantially above the experimental values. There are several possible causes for this disagreement. Assumption (6), that the light remains at normal incidence even after multiple reflections, may not be realistic. However, the assumption appears to be supported by the good agreement at small N. More questionable is the validity of assumption (3), that the structure of the top of the valence band in the doped region can be described by the m^* appropriate for the heavy holes. As already mentioned, both the disorder introduced by heavy doping, and the small value of d can be expected to perturb significantly the density of states. The interplay of quantum-well effects and disorder, and its effect on the electronic structure is certainly of considerable physical interest, but it is a complex subject, beyond the scope of this work. We shall take here a more heuristic approach, and try to fit the theory to experiment by considering m^* to be a fitting parameter. It turns out that the data can be well fitted when m^* is a quarter of the heavy-hole mass, as indicated in Fig. 2 by open circles. It would not be surprising if the DOS near the band edge was quite different from that in the undoped material.

ACKNOWLEDGMENTS

The research described in this paper was performed by the Jet Propulsion Laboratory, California Institute of Technology, under contract with the U.S. National Aeronautics and Space Administration and under support from the Jet Propulsion Laboratory Director's Discretionary Fund.

*Present address: Department of Physics, California Institute of Technology, Pasadena, CA 91109.

[1]E. E. Haller, M. R. Hueschen, and P. L. Richards, Appl. Phys. Lett. **34**, 495 (1979).

[2]For the temperature stabilization scheme, see J. W. V. Storey, Rev. Sci. Instrum. **52**, 769 (1981).

[3]D. M. Watson, Ph.D. thesis, University of California, Berkeley, 1982.

[4]P. P. Edwards and M. J. Sienko, Phys. Rev. B **17**, 2575 (1978).
[5]H. Y. Fan and M. Becker, in *Semiconducting Materials,* edited by H. K. Henisch (Buttersworths, London, 1951), p. 132.
[6]The fraction of light holes is very small, and they are therefore ignored.
[7]N. F. Mott and J. H. Davies, Philos. Mag. B **42**, 845 (1980).
[8]T. Ando, T. A. B. Fowler, and F. Stern, Rev. Mod. Phys. **54**, 437 (1982).
[9]J. R. Reitz, F. J. Milford, and R. W. Christy, *Foundations of Electromagnetic Theory,* 3rd ed. (Addison-Wesley, Reading, Mass., 1979), p. 349.
[10]J. R. Reitz, F. J. Milford, and R. W. Christy, Ref. 9, p. 403.
[11]T. H. Geballe, in *Semiconductors,* edited by N. B. Hannay (Reinhold, New York, 1959), p. 313.